Hindawi
Journal of Sensors
Volume 2020, Article ID 4575721, 11 pages
https://doi.org/10.1155/2020/4575721

Research Article

Dynamic Traffic Detection and Modeling for Beidou Satellite Networks

Yanyu Qu, Fangling Pu, Jianguo Yin, Lingzi Liu, and Xin Xu

School of Electronic Information, Wuhan University, Wuhan, Hubei 430072, China

Correspondence should be addressed to Fangling Pu; flpu@whu.edu.cn

Received 11 August 2019; Accepted 31 December 2019; Published 22 January 2020

Academic Editor: Grigore Stamatescu

Beidou navigation system (BDS) has been developed as an integrated system. The third BDS, BSD-3, will be capable of providing not only global positioning and navigation but also data communication. When the volume of data transmitted through BDS-3 continues to increase, BDS-3 will encounter network traffic congestion, unbalanced resource usage, or security attacks as terrestrial networks. The network traffic monitoring is essential for automatic management and safety assurance of BDS-3. A dynamic traffic detection method including traffic prediction by Long Short-Term Memory (LSTM) and a dynamically adjusting polling strategy is proposed to unevenly sample the traffic of each link. A distributed traffic detection architecture is designed for collection of the detected traffic and its related temporal and spatial information with low delay. A time-varying graph (TVG) model is introduced to represent the dynamic topology, the time-varying link, and its traffic. The BDS-3 network is simulated by STK. The WIDE dataset is used to simulate the traffic between the satellite and ground station. Simulation results show that the dynamic traffic detection method can follow the variation of the traffic of each link with uneven sampling. The detected traffic can be transmitted to the ground station in near real time through the distributed traffic detection architecture. The traffic and its related information are stored by using Neo4j in terms of the TVG model. The nodes, edges, and traffic of BDS-3 can be quickly queried through Neo4j. The presented dynamic traffic detection and representation schemes will support BDS-3 to establish automatic management and security system and develop business.

1. Introduction

Beidou is one of the most rapidly developing global navigation satellite systems (GNSS). China's Beidou navigation system has evolved from BDS-1, then BDS-2, to now BDS-3 in built [1]. The position precision of BDS has been improved rapidly, and its coverage of navigation services has also been expanded from Asian-Pacific regions to worldwide [2]. Besides navigation and positioning, BDS has also provided a short message communication [3, 4]. The short message communication has been demonstrated as an effective communication method in the area where the ground communication facilities did not cover or could not work. The in-construction BDS-3 has been equipped with the intersatellite link (ISL) in Ka-band and laser [5]. BDS will be an integrated satellite network which provides not only the fundamental positioning, navigation, and timing services but also short message communication and future wide-band multimedia communication [1]. A variety of application data will be transferred by BDS. BDS will encounter the problem of network traffic congestion when more communication services are uploaded to it and transferred by it. Dynamic traffic control is essential to secure BDS and enhance its resource utilization. Traffic monitoring and representation are two important mechanisms to realize dynamic traffic management and control. Compared with terrestrial networks, BDS has a dynamic topology and is operated automatically. The problem arises as to how to monitor and represent the traffic of BDS so that the network traffic can be captured in time. Our research focuses on the traffic monitoring of BDS-3 for business expansion.

BDS-3 is a hierarchical space network that is composed of 3 geostationary orbit (GEO) satellites, 3 inclined geosynchronous orbit (IGSO) satellites, 24 medium earth orbit (MEO) satellites, some additional satellites in orbit for backups or tests, and ground stations [1]. The ground stations consist

of the master control station (MCS), monitor stations (MS), and uplink stations (ULS). The link in this paper means the light of sight (LOS) communication between two nodes of BDS-3. The links that serve for data communication can be divided into two categories, the ground-satellite link (GSL) and ISL. Besides the traditional L-band, S-band, and C-band [5], newly developed wide bands, such as Ka-band and Laser, are utilized in GSLs [6]. Ka-band is also the main communication band of ISL. In the near future, laser will take more communication tasks than Ka-band in ISL [7]. Because each satellite of BDS-3 has its orbit [2], the link between two satellites is intermittent, and the capacity of communication also changes with the distance of the link. The topology of BDS-3 changes with a period. There are various topologies in a circle. The difficulty is how to balance the tradeoff between the real time traffic monitoring and the few burdens added to the communication links of both GSL and ISL.

The network traffic is a snapshot of the whole links' traffic at a specified interval. The network traffic monitoring is divided into each link traffic monitoring. This nonrouter monitoring techniques [8] have two modes, namely, active and passive. Although active monitoring introduces probes into a link, the detection information is more accurate and needs less computation resource in the host system than passive monitoring. We present an active polling scheme to collect measurements of a link in BDS-3. The widely used network measurement tools include SNMP- (Simple Network Management Protocol-) based detecting, packet sniffing, and flow-based tools [9]. Considering that the satellite network has limited on-board processing ability and storage and that the hardware is hard to supplement, SNMP is utilized to collect and organize the information about network devices and links of BDS-3. Under SNMP architecture, the traffic detection architecture of BDS-3 and the polling strategy are two key points for the traffic measurement in terms of active monitoring mode.

The distributed detection architecture is utilized for automatic traffic detection under SNMP. Previous studies about satellite network routing have shown that the dynamic grouping strategy is better than the fixed strategy in the changing satellite constellations [10]. Under the dynamic group strategy, the satellites are grouped, and the group managers are selected according to the characteristics of the specific satellite network topology [9, 11–14]. The group managers are in charge of controlling, gathering, and distributing information to group members. We design the distributed traffic detection architecture for BDS-3 according to the satellite orbits and visible time to the ground station.

There are two polling strategies to detect the traffic of a link, fixed-period polling and dynamic polling. The advantage of fixed-period polling is easy control and operation. However, it may result in waste of communication and storage resources, and low efficiency [15]. Under the dynamic polling strategy, the next polling interval is adjusted based on previous detected data. The dynamic polling strategy consists of two steps, traffic prediction and polling period adjustment. In the traffic prediction, the detected historical traffic data are used to predict the traffic of the next time point. The next polling period is adjusted based on the variation of traffic values in terms of the polling period adjustment strategy. The dynamic polling strategy can minimize the interference to the communication of links and reduce the cost of wireless transmission and storage.

The prediction algorithms commonly used in the polling dynamic strategies of terrestrial networks are statistical analysis methods, such as the linear regression model [16] and Markov chains [17, 18], and machine learning methods such as SVR (Support Vector Regression) [15]. The proposed traffic prediction algorithms are mainly ARMA (Autoregressive Moving Average) [19] and neural networks that include BPNN (Back Propagation Neural Network), RFBNN (Radial Basis Function Neural Network) [20], ESN (Echo State Network) [21], RNN (Recurrent Neural Network) [22], and LSTM [23]. Because the traffic detection algorithm should run on satellite systems, we choose the prediction algorithm in consideration of both the ability of computation and storage of satellite systems and the accuracy of prediction.

The polling period adjustment strategy determines how to adjust the next polling period if the predicted variation exceeds the thresholds [15, 16, 24]. The dynamic polling strategy makes the time at which the traffic is detected different from one link to another. A time alignment algorithm should be applied to synchronize the traffic of different links in order to compute the whole network traffic at specified intervals. The widely used time alignment methods are Lagrange interpolation, piecewise linear interpolation, and cubic spline interpolation.

The changing topology and the varying traffic of BDS-3 can be modeled by a time-varying graph (TVG) [25, 26]. TVG was developed from a static graph that was largely used to model network entities and their relations in the form of vertices and edges. TVG maps states of the graph at different times. TVGs have three mapping approaches, namely, the snapshot, the log file, and the whole-graph method, respectively. In the snapshot method, each graph snapshot is a static representation of a network at a time point. The log file method is a modified snapshot method whereby each historical snapshot with a timestamp is recorded and stored in a log file. The whole-graph method records each kind of network elements (i.e., vertex, edge, or attribute) with a valid time point or a valid time interval. After analyzing the three kinds of TVGs and the characteristics of BDS-3, we choose the whole-graph method to model the dynamic BDS-3. With the BDS-3 TVG model, the detected traffic of links and the corresponding network topology can be stored. The whole network traffic and its evolution can be derived. The TVG information is essential for BDS-3 management and traffic load balancing.

This paper focuses on the network traffic monitoring, collection, and representation with the aim of detecting and storing the network traffic of BDS-3 in time. It has three contributions. The first one is that a dynamic traffic polling scheme is proposed for detecting the traffic of a link. The second is that a TVG in terms of the whole-graph method is used to model the dynamic satellites, the topology, and the traffic of BDS-3. The third is that a distributed network traffic detection architecture in terms of SNMP was introduced for BDS-3.

The rest of this paper is organized as follows. In section 2, the methodology for network traffic detection, collection, and representation of BDS-3 is introduced. The methodology includes a dynamic traffic polling scheme, a distributed traffic detection architecture and a time-varying graph model. The simulation scenarios and their results are shown in section 3. The conclusion of our work is in section 4.

2. The Dynamic Traffic Detection, Representation, and Collection for BDS-3

The network traffic detection, representation, and collection framework are proposed based on the satellites, their orbits, and functions in BDS-3. GEO and IGSO satellites function not only as navigation systems but also as relays which forward space-based measurement and control information [6, 27]. Because the inclined orbit angle of IGSO is more than 0°, it is visible at high-latitude area. IGSO is more favorable than GEO for the MEO information relaying [27] in the designed distributed traffic detection architecture.

2.1. The Dynamic Traffic Polling Scheme. The dynamic polling scheme consists of two parts: (1) the data prediction algorithm and (2) the polling period adjusting strategy [15–18]. The block diagram of our dynamic polling scheme is depicted as Figure 1.

2.1.1. Traffic Prediction with LSTM. Assume that in the interval $[t_1, t_m]$, there are m detected traffic points $x(t_1), x(t_2), \cdots, x(t_m)$, where $t_1 < t_2 < \cdots < t_m$. Before input to LSTM, the unevenly spaced detected traffic series should be interpolated to an evenly spaced time series with the time step of T_s. So, an interpolation algorithm should be introduced. A cubic spline interpolation function $S(t)$ that satisfies $S(t_i) = x(t_i)$, $(i = 1, 2, \cdots, m)$, is a third-degree polynomial on each subinterval $[t_1, t_{i+1}]$, where $i = 1, 2, \cdots, m-1$. So that, $S(t)$ is a piecewise function:

$$S(t) = \begin{cases} s_1(t), & t_1 \le t < t_2, \\ s_2(t), & t_1 \le t < t_3, \\ \vdots & \\ s_{m-1}(t), & t_{m-1} \le t < t_m, \end{cases} \tag{1}$$

where $s_i(t)$ is a determined polynomial on each subinterval as

$$s_i(t) = a_i(t - t_i)^3 + b_i(t - t_i)^2 + c_i(t - t_i) + d_i. \tag{2}$$

The value of a_i, b_i, c_i, d_i is uniquely determined based on the property of interpolation continuity, differential continuity, and natural boundary conditions.

We sample the continuous interpolation curve $S(t)$ with the step of T_s. Then, we obtain an evenly spaced traffic time series $\bar{x} = \{\bar{x}(t_1), \bar{x}(t_2), \cdots, \bar{x}(t_n)\}$ whose length is $n = ((t_m - t_1)/T_s) + 1$, and it satisfies

$$\bar{x}(t_j) = S(t_j), \quad t_j = t_1 + (j-1) \cdot T_s, \tag{3}$$

where $j = 1, 2, \cdots, n$.

The time series $\bar{x} = \{\bar{x}(t_1), \bar{x}(t_2), \cdots, \bar{x}(t_n)\}$ is inputted to the trained LSTM model in order to predict the value of the next time point $t_{n+1} = t_n + T_s$. Then, the LSTM model outputs the predicted next traffic value $\hat{\bar{x}} = (t_{n+1})$.

We used historical traffic to train a LSTM model, and then utilized the trained model to predict traffic. LSTM is acknowledged as the state-of-art prediction model for time series prediction [28]. Our LSTM model consists of one recurrent hidden layer and one output layer. The block diagram of our LSTM model is shown in Figure 2.

The basic unit of the hidden layer is the LSTM neuron [29] which consists of one memory cell, one input gate, one output gate, one forget gate, and three adaptive and multiplicative blocks. The structure of an LSTM neuron is shown in Figure 3.

The memory cell c_t acts as an accumulator of the state information [30]. The input gate i_t and the output gate o_t control the input and output activations of the memory block, respectively. The forget gate f_t controls whether the past memory cell c_{t-1} is propagated to the current memory cell c_t. Assume the input of the model is $\{x_1, x_2, \cdots, x_t\}$, where x_t is a time series which is a slice of the evenly spaced detected traffic time series $\bar{x} = \{\bar{x}(t_t), \bar{x}(t_{t+1}), \cdots, \bar{x}(t_{t+k})\}$ introduced previously. The equations of the LSTM neuron are listed as follows:

$$\begin{aligned} i_t &= \sigma(\mathbf{W}_{xi}x_t + \mathbf{W}_{hi}h_{t-1} + \mathbf{W}_{ci}c_{t-t} + \mathbf{b}_i), \\ f_t &= \sigma(\mathbf{W}_{\mathrm{xf}}x_t + \mathbf{W}_{\mathrm{hf}}h_{t-1} + \mathbf{W}_{\mathrm{cf}}c_{t-1} + \mathbf{b}_f), \\ c_t &= f_t * c_{t-1} + i_t * \tanh(\mathbf{W}_{\mathrm{xc}}x_t + \mathbf{W}_{\mathrm{hc}}h_{t-1} + \mathbf{b}_c), \\ o_t &= \sigma(\mathbf{W}_{\mathrm{xo}}x_t + \mathbf{W}_{\mathrm{ho}}h_{t-1} + \mathbf{W}_{\mathrm{co}}c_t + \mathbf{b}_o), \\ h_t &= o_t * \tanh(c_i), \end{aligned} \tag{4}$$

where $\sigma(\cdot)$ and $\tanh(\cdot)$ represent the sigmoid function and hyperbolic tangent activation function, respectively. $\mathbf{W}$ represents weight matrices, and $\mathbf{b}$ represents bias vectors. The symbol $*$ denotes the Hadamard product. The output layer is a dense layer to make a single value prediction. The output h_t of the hidden layer is propagated to the output layer, and then, the predicted traffic $\hat{y}_t$ is obtained. During the process of dynamic polling, the parameters of the LSTM model are fine-tuned by the k latest traffic training samples. The training samples are interpolated from the real traffic series detected in the most recent period of time.

2.1.2. Dynamic Polling Period Adjusting Strategy. The next polling period is adjusted dynamically according to the variation of traffic. The period is extended if the variation is low, while the period is shortened if the variation is high.

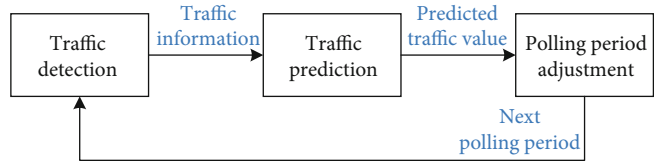

Figure 1: The block diagram of the dynamic polling scheme.

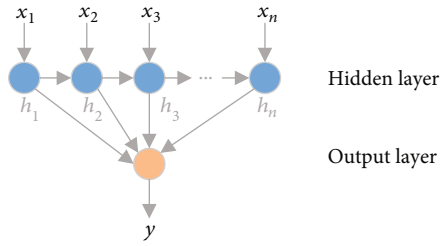

Figure 2: The block diagram of the LSTM model.

The rate of traffic change is decided by the latest detected traffic, and the next predicted traffic obtained by LSTM:

$$\delta = \frac{\left|\hat{\bar{x}}(t_{n+1}) - \bar{x}(t_n)\right|}{\bar{x}(t_n)}. \tag{5}$$

Assume the maximum period is $T_{\max}$, and the minimum period is $T_{\min}$. The maximum period is set to assure that the detector can poll at least once in the connection time of links, so $T_{\max}$ is set less than the minimum link duration of BDS. The minimum period assures that the polling does not take much network resources, so $T_{\min}$ is usually set to few seconds [17]. The adjusting factor ε is a number greater than one, which determines the adjusting step size. The upper threshold is $U_{\max}$, and the lower threshold is $U_{\min}$. The polling cycle of the next polling T_{n+1} is determined by the following procedures.

(i) Input the last k interpolated traffic values $\bar{x} = \{\bar{x}(t_{n-k+1}), \bar{x}(t_{n-k+2}), \cdots, \bar{x}(t_n)\}$ to LSTM to get the predicted value $\hat{\bar{x}}(t_{n+1})$ of the next time point $t_{n+1} = t_n + T_s$. Then calculate the rate of change δ by Equation (5)

(ii) Adjust the polling cycle according to ε. If $\varepsilon > U_{\max}$, then $T_{n+1} = \varepsilon T_n$. If $\varepsilon > U_{\min}$, then $T_{n+1} = T_n/\varepsilon$

(iii) Correct T_{n+1} in terms of bounds. If $T_{n+1} > T_{\max}$, then $T_{n+1} = T_{\max}$. If $T_{n+1} < T_{\min}$, then $T_{n+1} = T_{\min}$

(iv) Start the next polling after the time period of T_{n+1}, then renew the traffic series $\bar{x}$. Return to step (i) to restart next polling period adjustment

2.1.3. Total Traffic Estimation. The total traffic of the network is defined as the sum of all the link traffic at a time point. However, the traffic of different links is sampled asynchronously under the dynamic polling strategy. So, in the same period of time, both time points and the total amount of traffic samples are different from one link to another. The traffic samples of the three links are shown in Figure 4. Therefore, in order to calculate the total network traffic, we should align the timing-mismatched traffic sampling points to the same time points.

Considering that we want to get the total network traffic at time t, we align the traffic of each link by means of linear interpolation. Assume that the detected traffic of link j is $x_j = \{x_j(t_1), x_j(t_2), x_j(t_{N_j})\}$. The stepwise linear interpolation function $S_j(t)$ meets the conditions:

$$S_j(t) = \begin{cases} s_{j1}(t), & t_1 \le t < t_2, \\ s_{j2}(t), & t_2 \le t < t_3, \\ \vdots & \\ s_{j(N_{j-1})}(t), & t_{N_{j-1}} \le t < t_{N_j}, \end{cases} \tag{6}$$

where $s_{ji}(t)$ is a determined polynomial on each subinterval by

$$s_{ji}(t) = \frac{x_j(t_{i+1}) - x_j(t_i)}{t_{i+1} - t_i} t + \frac{x_j(t_i)t_{i+1} - x_j(t_{i+1})t_i}{t_{i+1} - t_i} \tag{7}$$

After obtaining the interpolation curve of each link, the total network traffic at any time t is computed by

$$x(t) = \sum_j S_j(t) \tag{8}$$

2.2. Distributed Traffic Detection Architecture for BDS-3. We designed an architecture for traffic collection and management of BDS-3 according to both SNMP protocol and satellites of BDS-3. There are 3 key components in SNMP, managed devices, agents, and network management systems (NMSs) [8]. The agent is a software that is installed on a managed device. Processing and memory resources are installed in NMSs. NMSs query agents for information and control and monitor the managed devices. In BDS-3, MEOs are agent satellites, while the ground stations are NMSs. Because IGSO satellites are almost visible to the ground stations, we assign MEO satellites and links information collection to IGSO satellites with the aim to shorten the time of information collection of all the satellites. Through the relay of IGSO satellites, the traffic information of BDS-3 can be transmitted to the ground stations in near real time. To distinguish IGSO satellites from the ground stations, we named IGSO satellites as detectors.

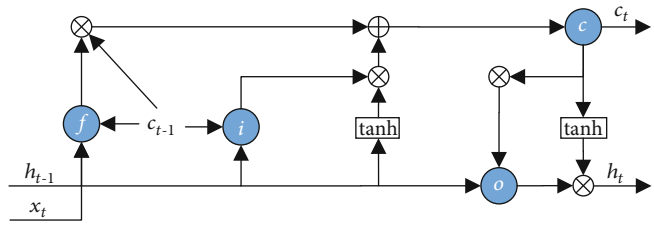

Figure 3: The structure of an LSTM neuron.

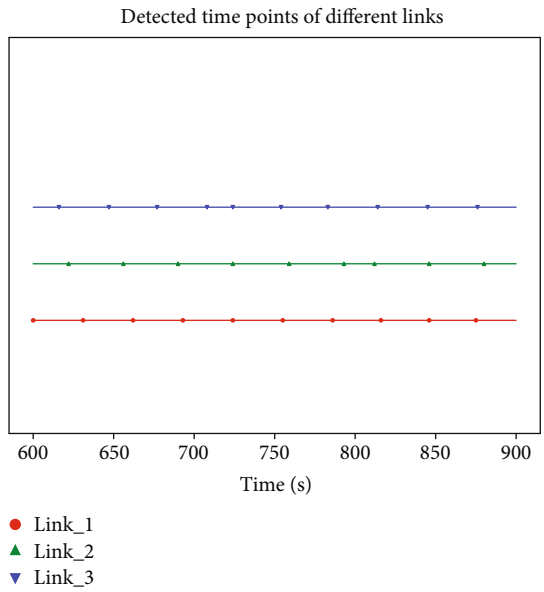

Figure 4: The sampling time points of different links.

Figure 5 shows the distributed detection architecture and the message transmission direction. The agent satellites are allocated to detector satellites in terms of the shortest route principle. The detection mechanism under the distributed detection architecture is described as follows. To begin with, the detector satellites, respectively, send request messages to the agent satellites in their coverage. Then, the agent satellite responds messages containing traffic information to the detector satellites. Next, the detector satellites forward the collected information to the ground station. The detector satellites can exchange their collected information if needed.

Under the distributed traffic detection architecture, the tasks of agent satellites' monitoring, traffic collection, and management are assigned to different IGSO satellites, so that the whole network operation states can be detected in near real time.

2.3. The Time-Varying Graph for a Satellite Network. We applied TVGs to describe a dynamic satellite network and its traffic. A graph model is designed to depict the topology, node and link attributes, and traffic that change over time. The changes of network topology and links are periodical and discrete, so finite periodic snapshots are applied to

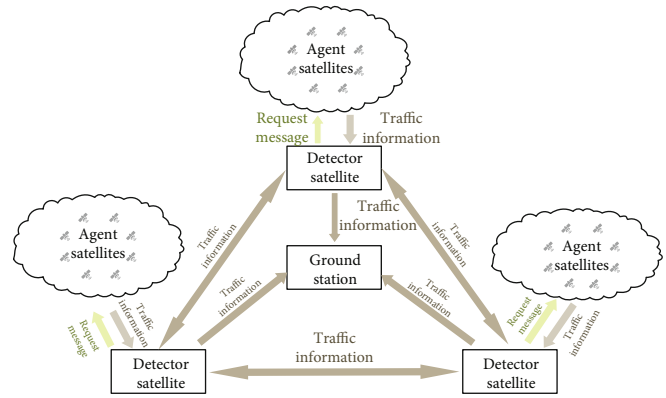

Figure 5: The distributed traffic detection architecture.

describe them. The change of link traffic is continuous, so an ever-extending time series are applied to depict it. The time-varying graph of a satellite network is expressed as $G = (V, E, S, \Gamma)$, which has the following components.

(i) $V = \{v_1, v_2, \cdots, v_n\}$: a set of n nodes (satellites and ground stations)

(ii) $E = \{e_1, e_2, \cdots, e_{n(n-1)/2}\}$: a set of direct links edges (links) between the nodes

(iii) $S = \{s_1, s_2, \cdots\}$: a time series of total traffic on the network

(iv) Γ: the time span of the graph

In one period time of T, the graph is depicted by several slices which are cut off according to the change rules of the satellite network. The several slices in a period are expressed as a slice time series, $G(V, E, \Gamma) = \{G(V, E, \Gamma_1), G(V, E, \Gamma_2), \cdots, G(V, E, \Gamma_n)\}$, where $\Gamma_1 = [t_1, t_2), \Gamma_2 = [t_2, t_3), \cdots, \Gamma_n = [t_n, t_{n+1})$, where $\Gamma_1 \cap \Gamma_2 \cap \cdots \cap \Gamma_n = \Theta$, and $\Gamma_1 \cup \Gamma_2 \cup \cdots \cup \Gamma_n = T$. So, the snapshot of the topology of satellite network at any time point t is $G(V, E, t) = G(T, E, t + T)$. $G(V, E, S, \Gamma)$ describes the global information of network topology and total traffic. The detailed information of each node and edge is introduced in the following context.

The attribute set of nodes is expressed as $F_V = (p, l, \Gamma_i)$, which has the following components:

(i) $p(c, t) \rightarrow \{0, 1\}$: called node presence function, which indicates whether a given satellite or ground

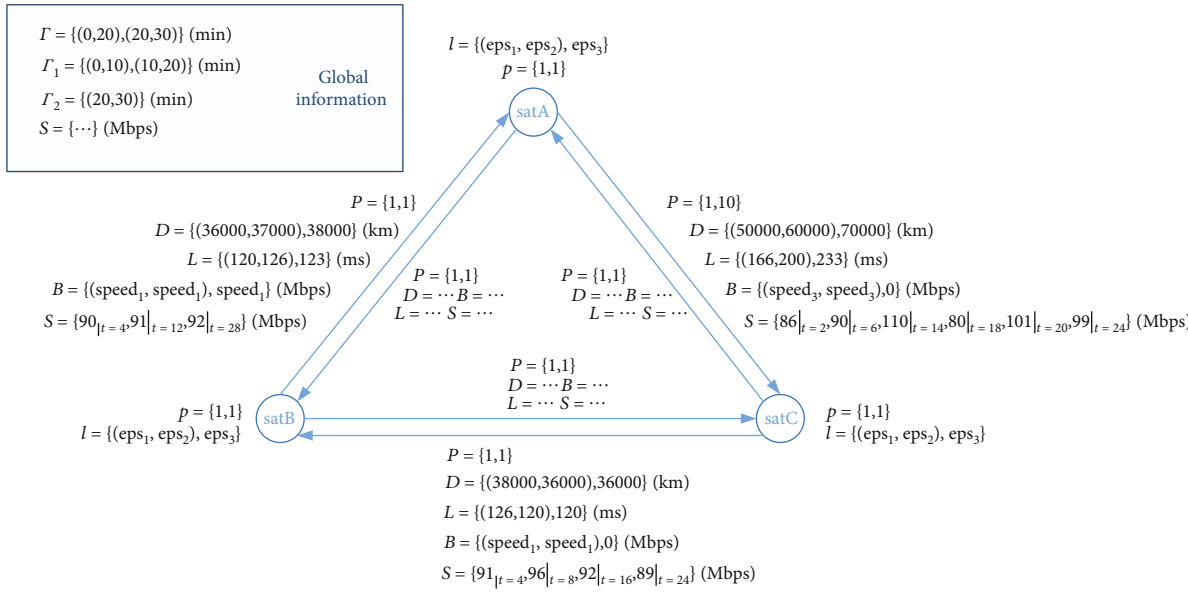

Figure 6: An example of time-varying graph for the satellite network.

station v is available at a given time t. The value of 1 is for available, 0 for unavailable

(ii) $l(v, t)$: called node position function, indicates the spatial position of a given node v at a given time t, which can be interpreted in the form of ephemeris parameters for a satellite, or GPS coordinate parameters for a ground station

The attribute set of edges is expressed as FE = (P, D, L, B, S, Γi), which has the following components:

(i) $P(e, t) \rightarrow \{0, 1\}$: called link presence function, which indicates whether a given link e exists at a given time t. The value of 1 means the link exists, while 0 means the link does not exist

(ii) $D(e, t)$: called link length function, which indicates the length of a given link e exists at a given time t. It is determined by the two nodes $s(v_1, t)$ and $s(v_2, t)$ at the ends of this edge

(iii) $L(e, t)$: called link latency function, which indicates the crossing time of a given link. It is proportional to link length $D(e, t)$

(iv) $B(e, t)$: called link bandwidth function, which is negatively related to link length $D(e, t)$

(v) $S(e, t)$: called link traffic function, which indicates the detected traffic of a given link e at a certain time t

After establishing the time-varying graph for a dynamic satellite network, the information of the satellite network can be well expressed. The snapshot of the network at any given time can be obtained, as well as the topology, link connectivity, link latency, and link traffic. Figure 6 shows an example of the TVG model of a satellite network, where satA, satB, and satC represents three MEOs, respectively.

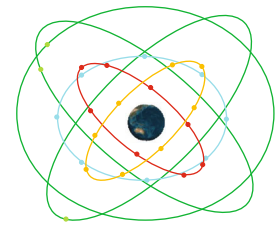

Figure 7: The IGSO/MEO constellation structure. Green orbits: IGSO. Red, blue, and yellow orbits: MEO.

3. Simulation and Results

3.1. Simulation Scenario Establishment. We established simulation scenarios by using STK (Satellite Tool Kit) tools. We simulated the dual-layer satellite network that was composed of 24 MEOs in standard Walker constellation 24/3/1, 3 IGSOs with phase difference of 120°, and 3 ground stations in China [5, 27]. The simulated constellation structure of the satellite network is shown in Figure 7.

The visibility between all the satellites and the ground station in Sanya is shown in Figure 8. As shown in Figure 8, the IGSO satellites keep links with the ground station, while the MEO satellites intermittently connect with the ground station. In our distributed traffic detection framework, the 3 IGSO satellites were designed as the detectors. The 24 MEO satellites were dynamically assigned to one of the 3 detectors according to Dijkstra's shortest path principle. Most of its orbit cycle time, a MEO satellite could find an IGSO satellite to relay the data to the ground station. If the

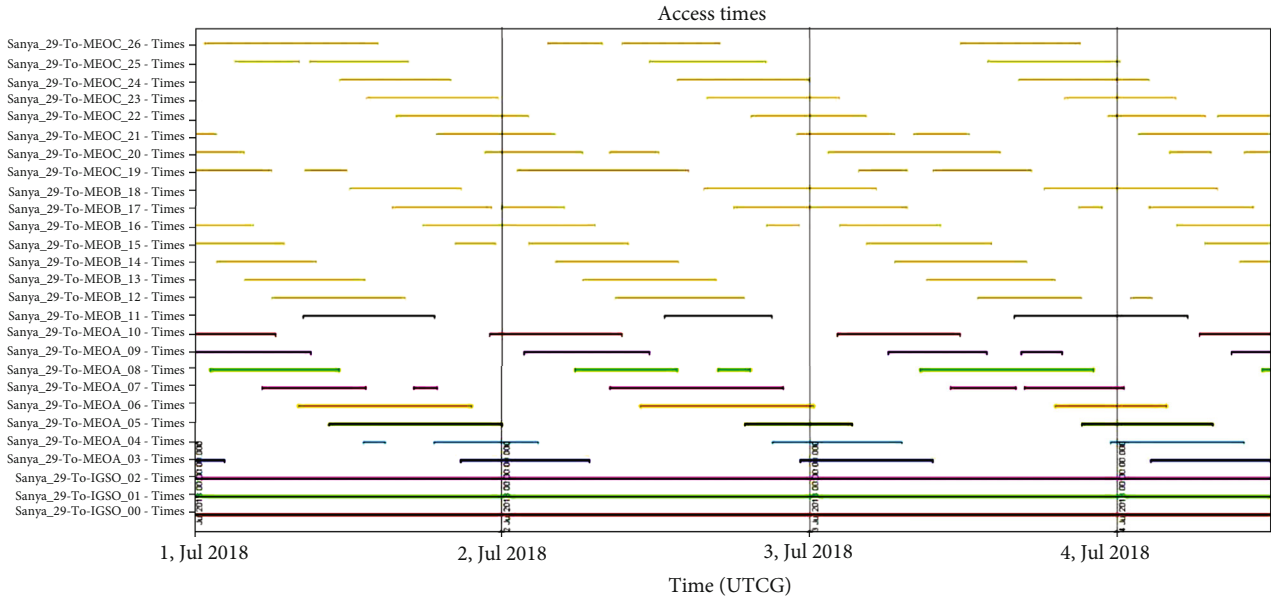

Figure 8: The visibility between two nodes of BDS-3.

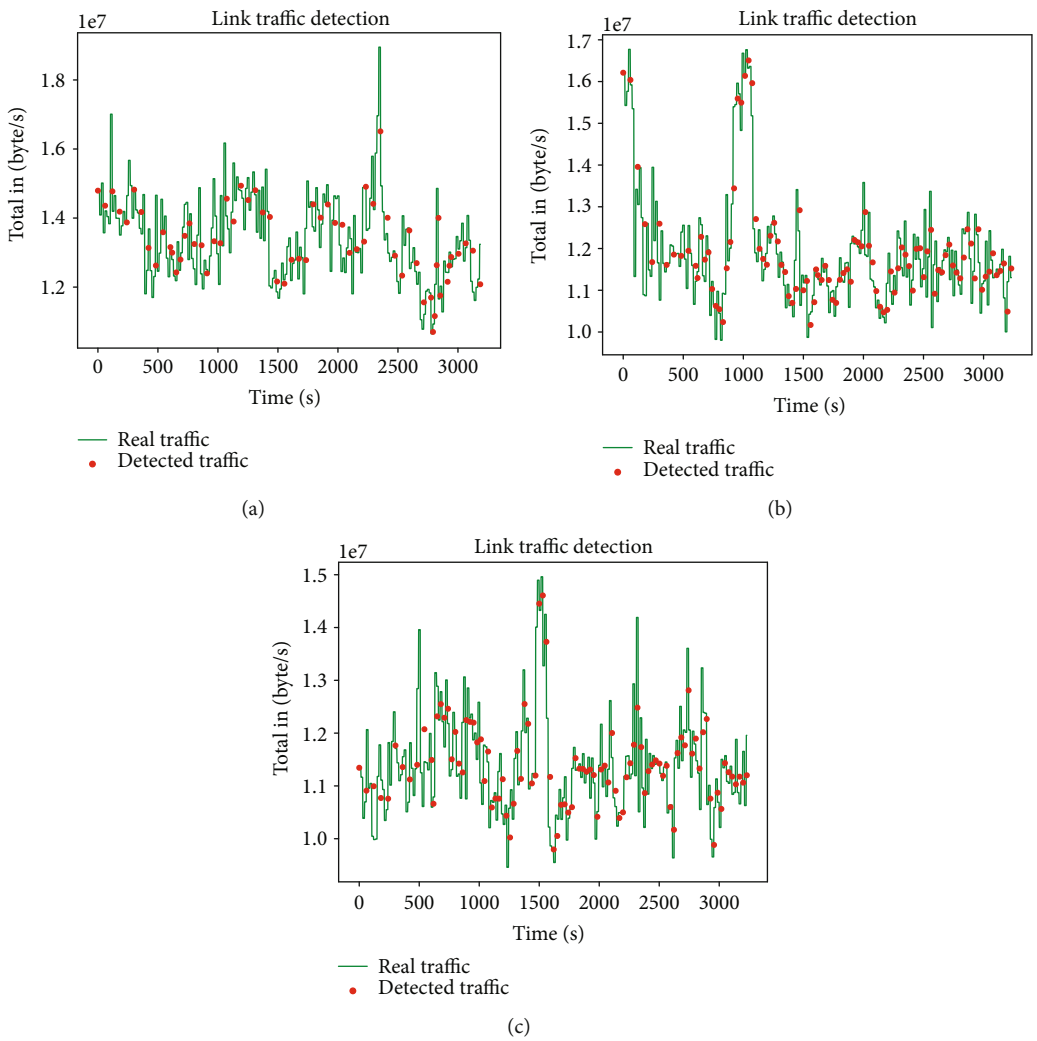

Figure 9: Results of dynamic traffic detection (a), (b), and (c), respectively, represent 3 different links.

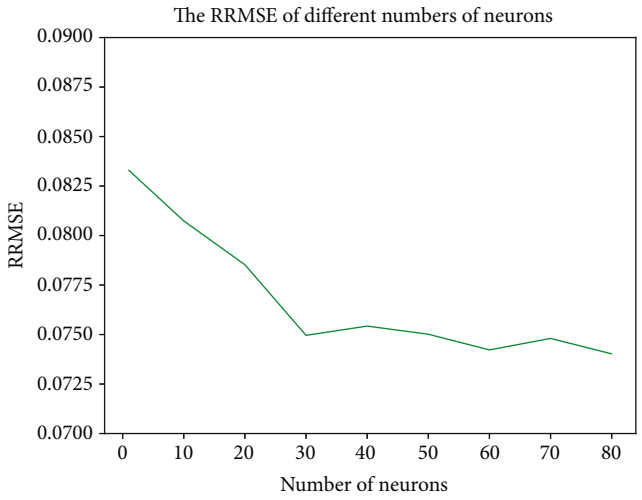

Figure 10: The RRMSE of different numbers of neurons.

traffic detection framework is centralized and the ground stations are selected as NMSs under SNMP protocol, the total connectivity time between the Sanya station and MEO 03 satellite (as an example) is 32 h during an orbit cycle of 84 h. Under the distributed traffic detection architecture that we presented, the total connectivity time between the MEO 03 and Sanya station through IGSO satellite relay is 82 h. Our distributed traffic detection framework reduces the interval to obtain the traffic of whole links because the time spent on the traffic detection of each link is largely shortened.

The link length l_{link} can be obtained through STK analysis of the established simulation scenarios. The link latency t_{link} is calculated as

$$t_{\text{link}} = \frac{l_{\text{link}}}{c} \tag{9}$$

where c represents the velocity of transmission. The latency spent on transmitting request messages or traffic response messages in the process of traffic detection can be calculated according to the result of Equation (9).

3.2. Results of Dynamic Traffic Detection. Assume the satellite-ground link is a laser link with a 150 Mbps rate [31]. In order to test the dynamic traffic detection method, we used the WIDE traffic dataset in the period between 2009/03/30, 00:00 and 09:00 as the traffic of the link between an IGSO satellite and a ground station. The average rate of this dataset is 92 Mbps, which is less than 150 Mbps. So, the WIDE dataset was considered a reasonable virtual traffic of the detector-ground links. We cut the WIDE dataset into several slices to represent the traffic of three detector-ground links. In the dynamic polling period adjusting strategy, the minimum polling period was set as 15 s in order to save network resources. So, the time resolution of the detected traffic time series is 15 s. Figure 9 shows the traffic sampling points and the traffic detection values of three simulated detector-ground links.

Table 1: Prediction performance of different methods.

	Link 1	Link 2	Link 3
RRMSE of ARMA	0.095	0.095	0.107
RRMSE of LSTM	0.077	0.073	0.084

Table 2: CPU and memory usage of dynamic polling using different prediction methods.

	Normal state	Dynamic polling with LSTM running	Dynamic polling with ARMA running
CPU usage	20.3%	31.8%	27.0%
Memory usage	34.1%	37.3%	37.6%

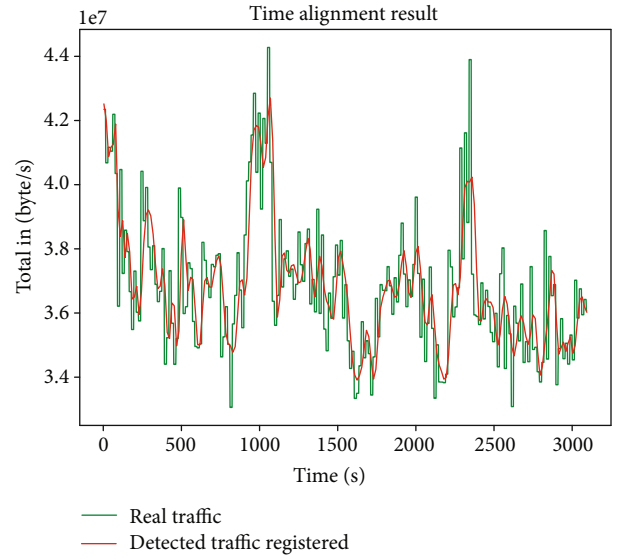

Figure 11: Results of total traffic estimation.

Table 3: Results of total traffic estimation using different interpolation methods.

Interpolation method	Linear	Nearest	Cubic spline
RRMSE	0.036	0.040	0.037

Assuming that the sampling number is N, the predicted traffic value of every polling round is expressed as $\{\hat{y}(t_1), \hat{y}(t_2), \cdots, \hat{y}(t_n)\}$, the corresponding real traffic value is $\{y(t_1), y(t_2), \cdots, y(t_n)\}$. The relative root mean square error (RRMSE) defined in Equation (10) is utilized to measure the prediction performance of LSTM.

$$\text{RRMSE} = \sqrt{\frac{\sum_{i=0}^{N}((y\wedge(i) - y(i))/y_i)^2}{N}}. \tag{10}$$

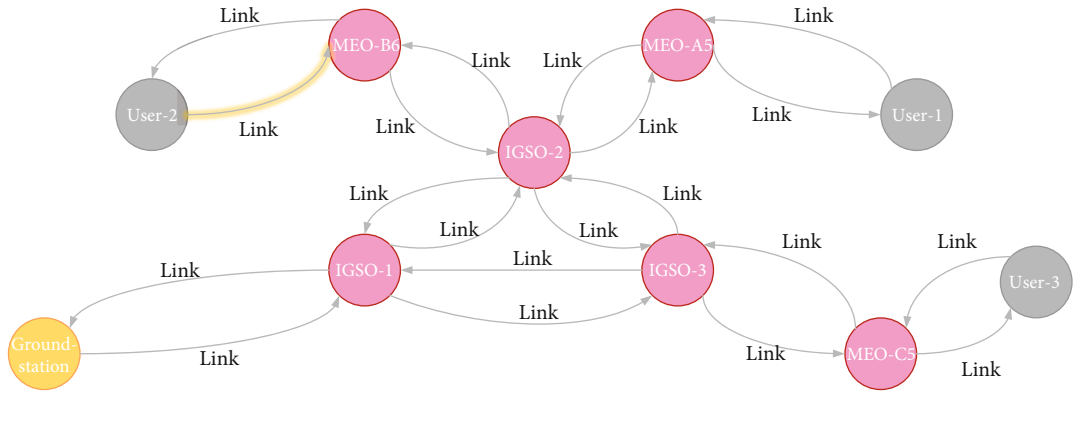

Figure 12: A snapshot of the BDS-3 TVG model stored in the Neo4j database.

Because the number of neurons in the hidden layer of the LSTM model can influence the prediction performance, experiments were conducted to determine the number of neurons of the dynamic traffic polling. As illustrated in Figure 10, the descent speed of RRMSE is fast before 30 neurons and is slow even fluctuant after 30 neurons. The more neurons, the more is the complexity and computation cost. So, we chose a 30-neuron hidden layer for the tradeoff between performance and complexity.

The traffic prediction performance of LSTM was compared with ARMA (2,1) [32] which is a conventional traffic prediction method used in satellite networks. Considering the limited on-board computational power and storage, the CPU usage and memory usage of the dynamic traffic polling schemes using different prediction methods were also compared. The experiments run on a personal computer with Intel Core i54570 (3.20 GHz), 16 GB, 64-bit operating system Windows 10. The prediction performances of ARMA and LSTM are shown in Table 1. LSTM has less RRMSE than ARMA in traffic prediction. LSTM improves the accuracy of traffic prediction. The CPU usage and memory usage of dynamic traffic polling using ARMA and LSTM are, respectively, shown in Table 2. The dynamic traffic polling scheme with LSTM has a little less memory consumption and a little more CPU usage than that with ARMA. We found that LSTM has been used in the satellite system for on-board task planning [33], which means the on-board computing resources can support for running LSTM. So, after a systematic consideration, LSTM instead of ARMA was chosen in traffic prediction of satellite links.

After dynamic traffic polling, the whole traffic that included the 3 links were estimated. The three time-mismatching detected traffic series were aligned by linear interpolation.

We estimated the total traffic per 15 s according to the time resolution of 15 s. The results of the total 3-link traffic are shown in Figure 11. In Figure 11, the estimated total traffic curve is similar to the real summed traffic curve.

RRMSE between the estimated total traffic curve and the real total traffic curve is computed to evaluate the estimation performance. We also tried another two interpolation methods, nearest and cubic spline, in the procedure of total traffic computation. The performance of total traffic estimation is listed in Table 3. It can be seen from Table 3 that there is little difference among the linear, nearest, and cubic spline methods. This reason may be that the estimation results mainly depend on the sampling series and they are not sensitive to the alignment method. Therefore, linear interpolation is chosen in order to save the calculation cost.

3.3. TVG Database. When the detected traffic and its related information, such as node and link attributes, and timestamps are transmitted to the ground stations, they are organized in terms of the introduced TVG model. We chose a graph database, Neo4j, to store the information of the TVG model of the simulated satellite network. We can query the information of a satellite or a link from the Neo4j database. We can also snapshot the traffic of the whole satellite network at a given time. One snapshot of a part of the satellite network is shown in Figure 12. The attributes and traffic information of the link highlighted in yellow are shown at the bottom of Figure 12. The information of the TVG model for BDS-3 can be well stored in the Neo4j database. The database supports quick query of the nodes, edges, and traffic in the BDS-3 system. Neo4j will be an efficient tool for BDS-3 management.

4. Conclusion

BDS-3 is being established as a GNSS. It is not only responsible for positioning and navigation but also for message communication and further data transmission. Traffic detection and representation are basic techniques for automatic management and control of BDS-3 with the aim of ensuring safety operation. Under the SNMP protocol, a dynamic traffic detection method including traffic prediction by LSTM and a polling adjusting strategy was proposed for detecting the traffic of each link in BDS-3. A distributed traffic detection architecture was also established to collect the traffic and its related information in near real time. A TVG model was introduced to represent the dynamic topology and the traffic of each link at specific times. We used STK to simulate

the BDS-3 and the WIDE dataset to simulate the traffic between IGSO satellites and the ground station. Simulation results show that our traffic detection method can track the variation of the traffic with nonuniform sampling and the detection error is low. The distributed traffic detection architecture avoids the influence of intermittence that is caused by characteristics of BDS-3 and shortens the time of information transmission from satellites to the ground station. Neo4j is utilized to store the obtained data that are organized by the TVG model, which results in quick query and the computation of the traffic of the whole satellite network. Our work will support BDS-3 to realize automatic management, security establishment, and business expansion.

Data Availability

The WIDE dataset was downloaded from the website, http://mawi.wide.ad.jp/mawi/ditl/ditl2009/ (Kenjiro Cho, Koushirou Mitsuya and Akira Kato, "Traffic Data Repository at the WIDE Project", USENIX 2000 FREENIX Track, San Diego, CA, June 2000). We have explained that we selected the data between 2009/03/30, 00 : 00 and 09 : 00. The dataset is an opensource. Previously reported (data type: Beidou orbits) data were used to support this study and are available at (DOI: 10.1007/s10291-018-0784-0, 10.1007/978-981-13-0005-9_4). These prior studies (and datasets) are cited at relevant places within the text as references [5, 27].

Conflicts of Interest

The authors declare that they have no conflicts of interest.

Acknowledgments

This work was supported by the National Key Research and Development Program of China under Grant No. 2018YFB2100503. It was also supported by the Thirteen-five Civil aerospace planning project—integration and application of communication, navigation and remote sensing.

References

[1] Y. Yang, W. Gao, S. Guo, Y. Mao, and Y. Yang, "Introduction to beidou-3 navigation satellite system," *Navigation*, vol. 66, no. 1, pp. 7–18, 2019.

[2] X. Li, X. Zhang, X. Ren, M. Fritsche, J. Wickert, and H. Schuh, "Precise positioning with current multi-constellation Global Navigation Satellite Systems: GPS, GLONASS, Galileo and BeiDou," *Scientific Reports*, vol. 5, no. 1, article 8328, 2015.

[3] Y. Gong, S. Fan, L. Luo, and X. Liu, "Research on the online monitoring data transmission technology based on beidou communication," in *2018 IEEE 18th International Conference on Communication Technology (ICCT)*, pp. 660–663, Chongqing, China, October 2018.

[4] Q. Liu, Y. Chen, H. Hu, J. Jiang, Z. Ni, and X. Li, "The application of beidou satellite communication in drifting buoys," in *2018 International Conference on Sensing,Diagnostics, Prognostics, and Control (SDPC)*, pp. 715–718, Xi'an, China, August 2018.

[5] Y. Zhou, Y. Wang, W. Huang, J. Yang, and L. Sun, "In-orbit performance assessment of beidou intersatellite link ranging," *GPS Solutions*, vol. 22, no. 4, p. 119, 2018.

[6] M. Gregory, F. Heine, H. Kampfner, R. Meyer, R. Fields, and C. Lunde, "Tesat laser communication terminal performance results on 5.6Gbit coherent inter satellite and satellite to ground links," in *Proceedings Volume 10565, International Conference on Space Optics — ICSO 2010*, Rhodes Island, Greece, November 2017.

[7] S.-K. Liao, H.-L. Yong, C. Liu et al., "Long-distance free-space quantum key distribution in daylight towards inter- satellite communication," *Nature Photonics*, vol. 11, no. 8, pp. 509–513, 2017.

[8] A. Cecil, "A summary of network traffic monitoring and analysis techniques," *Computer Systems Analysis*, pp. 4–7, 2006.

[9] D. Zhou, Z. Yan, Y. Fu, and Z. Yao, "A survey on network data collection," *Journal of Network and Computer Applications*, vol. 116, pp. 9–23, 2018.

[10] W. Wang, G. Chen, S. Guo, X. Song, and Q. Zhao, "A study on the beidou igso/meo satellite orbit determination and prediction of the different yaw control mode," *China Satellite Navigation Conference (CSNC) 2013 Proceedings. Lecture Notes in Electrical Engineering, vol 245*, J. Sun, W. Jiao, H. Wu, and C. Shi, Eds., , pp. 31–40, Springer, Berlin, Heidelberg, 2013.

[11] X. Yi, Z. Sun, F. Yao, and Y. Miao, "Satellite constellation of MEO and IGSO network routing with dynamic grouping," *International Journal of Satellite Communications and Networking*, vol. 31, no. 6, pp. 277–302, 2013.

[12] X. Yi, Z. Hou, T. Zhong, Y. Zhang, and Z. Sun, "Route strategy of satellite network in gnss based on topology evolution law," *Journal of Systems Engineering and Electronics*, vol. 25, no. 4, pp. 596–608, 2014.

[13] X. Feng, M. Yang, and Q. Guo, "A novel distributed routing algorithm based on data-driven in geo/leo hybrid satellite network," in *2015 International Conference on Wireless Communications & Signal Processing (WCSP)*, pp. 1–5, Nanjing, China, October 2015.

[14] X. Qi, J. Ma, D. Wu, L. Liu, and S. Hu, "A survey of routing techniques for satellite networks," *Journal of Communications and Information Networks*, vol. 1, no. 4, pp. 66–85, 2016.

[15] Q. Sun, L. Gao, H. Wang, and X. Chao, "A dynamic polling strategy based on prediction model for large-scale network monitoring," in *2013 International Conference on Advanced Cloud and Big Data*, pp. 8–13, Nanjing, China, December 2013.

[16] W. B. Cao, G. S. Chen, G. Niu, and Z. Yang, "Monitoring technology of network devices based on ICMP and SNMP," *Computer Engineering & Design*, vol. 35, no. 4, 2014.

[17] H. Cai, M. Zhou, S. Jiang, and D. Han, "Application of polling strategy in space tt&c operation management systems," *Journal of Spacecraft TT&C Technology*, vol. 3, p. 10, 2013.

[18] Z.-h. Yang, Y. Wang, and R. Su, "Intelligent polling strategy for network management system," *Computer Engineering*, vol. 9, 2010.

[19] L. Chisci, R. Fantacci, and T. Pecorella, "Predictive bandwidth control for geo satellite networks," in *2004 IEEE International Conference on Communications (IEEE Cat. No. 04CH37577)*, pp. 3958–3962, Paris, France, June 2004.

[20] G. Zihe, G. Qing, and N. Zhenyu, "A distributed routing algorithm with traffic prediction in Leo satellite networks," *Information Technology Journal*, vol. 10, no. 2, pp. 285–292, 2011.

[21] H. X. Qin and F. Yang, "A new traffic flow prediction algorithm for satellite communication network," *Telecommunication Engineering*, vol. 53, no. 7, 2013.

[22] R. Vinayakumar, K. P. Soman, and P. Poornachandran, "Applying deep learning approaches for network traffic prediction," in *2017 International Conference on Advances in Computing, Communications and Informatics (ICACCI)*, pp. 2353–2358, Udupi, India, September 2017.

[23] X. Ma, Z. Tao, Y. Wang, H. Yu, and Y. Wang, "Long short-term memory neural network for traffic speed prediction using remote microwave sensor data," *Transportation Research Part C: Emerging Technologies*, vol. 54, pp. 187–197, 2015.

[24] S. R. Chowdhury, M. F. Bari, R. Ahmed, and R. Boutaba, "Payless: a low cost network monitoring framework for software defined networks," in *2014 IEEE Network Operations and Management Symposium (NOMS)*, pp. 1–9, Krakow, Poland, May 2014.

[25] A. Zaki, M. Attia, D. Hegazy, and S. Amin, "Comprehensive survey on dynamic graph models," *International Journal of Advanced Computer Science and Applications*, vol. 7, no. 2, pp. 573–582, 2016.

[26] I. Maduako and M. Wachowicz, "A space-time varying graph for modelling places and events in a network," *International Journal of Geographical Information Science*, vol. 33, no. 10, pp. 1915–1935, 2019.

[27] C. Li, X. Yi, Y. Zhao, and Z. Hou, "Research on space-based measurement and control scheme of launch vehicle based on BeiDou navigation satellite system," *China Satellite Navigation Conference (CSNC) 2018 Proceedings. CSNC 2018. Lecture Notes in Electrical Engineering, vol 497*, J. Sun, C. Yang, and S. Guo, Eds., , pp. 45–58, Springer, Singapore, 2018.

[28] Z. Chao, F. Pu, Y. Yin, B. Han, and X. Chen, "Research on real-time local rainfall prediction based on mems sensors," *Journal of Sensors*, vol. 2018, Article ID 6184713, 9 pages, 2018.

[29] W. Zhu, C. Lan, J. Xing et al., "Co-occurrence feature learning for skeleton based action recognition using regularized deep LSTM networks," in *Thirtieth AAAI Conference on Artificial Intelligence*, Phoenix, AZ, USA, March 2016.

[30] S. H. I. Xingjian, Z. Chen, H. Wang, D.-Y. Yeung, W.-K. Wong, and W.-c. Woo, "Convolutional LSTM network: a machine learning approach for precipitation nowcasting," in *Advances in Neural Information Processing Systems*, pp. 802–810, New York, USA, 2015.

[31] D. Wei, *Self-similar traffic prediction scheme for satellite internet services*, Master's thesis, Harbin Institute of Technology, 2014.

[32] Y. Dong and L. Wang, "Tpdr: traffic prediction based dynamic routing for leo&geo satellite networks," in *2015 IEEE 5th International Conference on Electronics Information and Emergency Communication*, pp. 104–107, Beijing, China, May 2015.

[33] S. Peng, H. Chen, C. Du, J. Li, and N. Jing, "Onboard observation task planning for an autonomous earth observation satellite using long short-term memory," *IEEE Access*, vol. 6, pp. 65118–65129, 2018.